



Optimized Combination of b-values for IVIM Perfusion Imaging in Acute Ischemic Stroke Patients

Guangming Zhu¹ · Jeremy J. Heit¹ · Blake W. Martin¹ · David G. Marcellus¹ · Christian Federau^{2,3} · Max Wintermark¹

Received: 25 May 2019 / Accepted: 11 July 2019 / Published online: 2 August 2019
© Springer-Verlag GmbH Germany, part of Springer Nature 2019

Abstract

Purpose To determine the optimal combination of low b-values to generate perfusion information from intravoxel incoherent motion (IVIM) in patients with acute ischemic stroke (AIS) considering the time constraints for these patients.

Methods A retrospective cohort study of AIS patients with IVIM MRI was performed. A two-step voxel-by-voxel postprocessing was used to derive IVIM perfusion fraction maps with different combinations of b values. Signal values within regions of ischemic core, non-infarcted ischemic hemisphere, and contralateral hemisphere were measured on IVIM (f , D^* , fD^* , D) parameter maps. Bland-Altman analysis and the Dice similarity coefficient were used to determine quantitative and spatial agreements between the reference standard IVIM (IVIM with 6 b values of 0, 50, 100, 150, 200, 1000/s/mm²) and other combinations of b values. Significance level was set at $p < 0.05$.

Results There were 58 patients (36 males, 61.3%; mean age 70.2 ± 13.4 years) included. Considering all IVIM parameters, the combination of b values of 0, 50, 200, 1000 was the most consistent with our reference standard on Bland-Altman analysis. The best voxel-based overlaps of ischemic regions were on IVIM D , while there were good voxel-based overlaps on IVIM f .

Conclusion The IVIM with these four b values collects diffusion and perfusion information from a single short MRI sequence, which may have important implications for the imaging of AIS patients.

Keywords MRI · Molecular diffusion coefficient · Pseudodiffusion coefficient · Flowing blood volume fraction · Multiple b-values

Guarantor The scientific guarantor of this publication is Dr. Max Wintermark.

Electronic supplementary material The online version of this article (<https://doi.org/10.1007/s00062-019-00817-w>) contains supplementary material, which is available to authorized users.

✉ Max Wintermark
max.wintermark@gmail.com

¹ Department of Radiology, Neuroradiology
Section, Stanford Healthcare, 300 Pasteur Drive –
S047, Stanford, CA 94305, USA

² Institute for Biomedical Engineering, ETH Zürich,
Gloriastrasse 35, 8092 Zürich, Switzerland

³ Department of Radiology, Diagnostic and
Interventional Neuroradiology, University of Basel,
Petersgraben, 4031 Basel, Switzerland

Abbreviations

ADC	Apparent diffusion coefficient
AIS	Acute ischemic stroke
ANOVA	Analysis of variance
CBF	Cerebral blood flow
CBV	Cerebral blood volume
CTA	Computed tomography angiography
D	Molecular diffusion coefficient
D^*	Pseudodiffusion coefficient
DWI	Diffusion-weighted imaging
f	Flowing blood volume fraction
FLAIR	Fluid-attenuated inversion recovery
GRE	Gradient echo
IVIM	Intravoxel incoherent motion
LVO	Large vessel occlusion
MRA	Magnetic resonance angiography
MRI	Magnetic resonance imaging
MTT	Mean transit time
NIHSS	National Institutes of Health Stroke Scale
PWI	Perfusion-weighted imaging

ROI Regions of interest
Tmax Time-to-Maximum

Key points

1. Intravoxel incoherent motion with optimized four b values enables collation of both diffusion and perfusion information from a single short MRI sequence.
2. Intravoxel incoherent motion may have important implications for the imaging of AIS patients.

Introduction

Intravoxel incoherent motion (IVIM) is a magnetic resonance imaging (MRI) perfusion technique that does not require the injection of a contrast agent [1]. It derives perfusion parameters from diffusion-weighted imaging (DWI) with multiple b-values, which offers the potential to assess both ischemic core infarction and perfusion in patients with acute ischemic stroke (AIS) [2–5]. With appropriate mathematical modelling, the following parameter maps can be derived: (1) f , which is related to vascular volume fraction, (2) D^* as the pseudodiffusion coefficient, which is related to microcapillary perfusion, (3) fD^* , which is related to blood flow, and (4) D , which is molecular diffusion coefficient. The IVIM f , D^* , and fD^* have been correlated to mean transit time (MTT), cerebral blood volume (CBV), and cerebral blood flow (CBF) MR perfusion maps, respectively (Table 1; [6]).

Although IVIM shows promise for cerebral perfusion evaluation in AIS patients [7], as a research tool it has not been well evaluated and was not the standard clinical MRI protocol. Also, there is no consensus as to the optimal b-values during IVIM acquisition for cerebral perfusion and ischemia measurement. The IVIM acquisitions may include more than 10 b-values from 0 to 3500, which include multiple low b-values from 0 to 200 to generate the IVIM perfusion parameter maps [8]; however, an increased number of b-values requires longer imaging time, which may introduce motion artifacts and delays in terms of AIS patient treatment.

In this retrospective cohort study, we sought to determine the variation in IVIM perfusion parameter maps as a function of the combination of b-values to generate in the setting of AIS due to anterior circulation large vessel occlusion (LVO) of the internal carotid artery or middle cerebral artery (M1 segment).

Material and Methods

Patient Enrolment and Demographic/Clinical Details

This single-center, retrospective cohort study was approved by our institutional internal review board, which waived patient consent. We searched our clinical and imaging database between 1 January 2016 and 30 April 2018 for patients admitted for suspected AIS. Inclusion criteria were: (1) presentation and MR imaging within 72 h of symptom onset; (2) magnetic resonance angiography (MRA) or computed tomography angiography (CTA) demonstrates anterior circulation LVO of the internal carotid artery or middle cerebral artery (M1 segment); (3) IVIM MR images obtained within 72 h of symptom onset. Patient demographic and clinical variables were recorded from the electronic medical record. Clinical variables recorded included: age, sex, hypertension, atrial fibrillation, diabetes mellitus, hyperlipidemia, National Institutes of Health Stroke Scale (NIHSS) on admission, and time since last seen normal at the time of MRI.

Image Acquisition and Postprocessing

Brain MRI was performed on a 3.0T GE MR750 MRI scanner using an 8-channel GE HR brain coil (GE Healthcare, Milwaukee, WI, USA). All MRI studies included DWI and IVIM. In some cases, additional sequences (Fluid-attenuated inversion recovery [FLAIR], gradient echo [GRE], perfusion-weighted imaging [PWI], MRA) were performed, but these sequences were not analyzed in the present study. Technical details and parameters for the sequences used in this study were as follows: DWI parameters: TR = 6000 ms, TE = 78.2 ms; b-value = 0

Table 1 Relation between IVIM and conventional diffusion/perfusion parameters

IVIM parameters and their definitions		Conventional diffusion/perfusion parameters
f	Perfusion fraction	CBV
D^*	Pseudodiffusion coefficient related to microcapillary perfusion	1/MTT or 1/Tmax
fD^*	The multiplication of f and D^* , related to blood flow	CBF
D	Molecular diffusion coefficient	DWI/ADC

CBV cerebral blood volume, MTT mean transit time, CBF cerebral blood flow, Tmax time-to-Maximum, DWI diffusion weighted imaging, ADC apparent diffusion coefficient

Table 2 Combinations of different b-values tested in this study

Group	Number of b-values	b-values (s/mm ²)
Reference standard	6 b values	0, 50, 100, 150, 200, 1000
Combination 1	5 b values	0, 100, 150, 200, 1000
Combination 2	5 b values	0, 50, 150, 200, 1000
Combination 3	5 b values	0, 50, 100, 200, 1000
Combination 4	4 b values	0, 150, 200, 1000
Combination 5	4 b values	0, 50, 200, 1000
Combination 6	4 b values	0, 100, 200, 1000
Combination 7	3 b values	0, 200, 1000

and 1000 s/mm²; flip angle 90°, and slice thickness of 5 mm. The IVIM was performed with an axial echoplanar DWI sequence (TR=4500 ms, TE=77 ms, field of view=240×240 mm², reconstruction matrix=128×128, slice thickness=5 mm, bandwidth=1953 Hz/pixel) with 6 b-values (0, 50, 100, 150, 200, 1000 s/mm²). The duration of IVIM acquisition was approximately 2 min and IVIM data were processed by an investigator who was blinded to the clinical analysis using a dedicated Matlab (MathWorks, Natick, MA, USA) code. A bi-exponential IVIM signal equation was fitted to generate f =perfusion fraction, coefficient D^* =pseudodiffusion coefficient, fD^* =the blood flow, and D =diffusion related IVIM parameter maps [6, 9].

The IVIM comparison groups were designated as follows: because several b-values are required for IVIM processing [7], we used b values of 0, 200 and 1000 s/mm² as our baseline 3 b values. Next, IVIM derived from 6 b values (0, 50, 100, 150, 200, 1000) was designated as the reference standard and 7 additional combinations (combinations 1–7)

of multiple b values (b=50, 100, 150) were then compared to the reference standard (Table 2).

Image Evaluation

All MR images were anonymized and reviewed on Horos (v2.1.1, Nimble Co LLC d/b/a Purview, Annapolis, MD USA) by a neurologist (GZ with 19 years of experience) and 2 neuroradiologists (MW with 21 years of experience, and JJH with 15 years of experience).

Regions of interest (ROI) were determined using DWI images as follows (Fig. 1): (1) ischemic core was defined as DWI hyperintense signal abnormality with a corresponding apparent diffusion coefficient (ADC) hypointense signal abnormality ($ADC < 620 \times 10^{-6} \text{ mm}^2/\text{s}$) [10]; (2) non-infarcted ischemic hemisphere was defined as the brain tissue with normal DWI signal on the ischemic side; (3) contralateral hemisphere was defined as the normal hemisphere contralateral to the ischemic one. The DWI images were manually outlined as these three ROIs on the slice with largest ischemic core in Horos, and the ROI were then overlaid

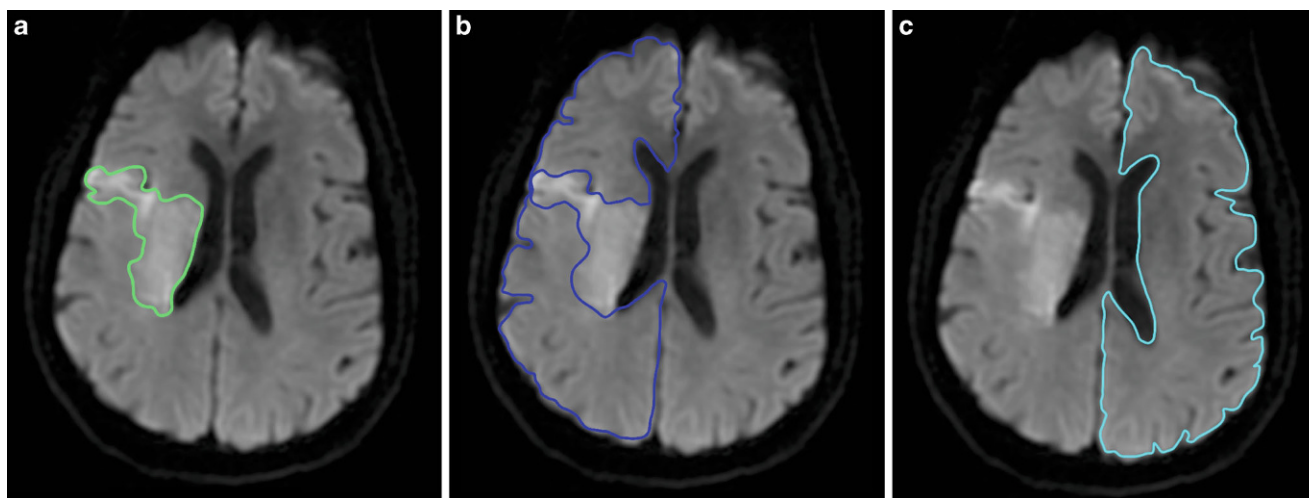


Fig. 1 Methods for defining regions of interest in this study. **a** Infarct core; **b** Non-infarcted hemisphere; **c** Contralateral hemisphere. Brain compartments are defined on one slice with the larger visible ischemic core. The ischemic core was defined based on restricted diffusion with apparent diffusion coefficient ($ADC < 620 \text{ mm}^2/\text{s}$). The non-infarcted ischemic hemisphere was defined as diffusion-weighted imaging (DWI) normal signal area at the infarcted hemisphere. Contralateral hemisphere was defined as the normal hemisphere contralateral to the hemisphere with infarction

on registered IVIM parameter f , D^* , fD^* and D maps for comparative measurements. The region-wise values of each IVIM parameter within these different ROIs were recorded.

The last step was to determine the differences between ischemic volumes delineated by optimized IVIM maps and reference standard. The ischemic area, which includes the ischemic core and penumbra, were visually segmented on all IVIM maps by a reader who was blinded to other routine MR images. Segmented regions were manually outlined as ROIs in Image J (Mac 1.51, National Institutes of Health, Bethesda, MD, USA) [11] and the volumes were calculated automatically. The spatial overlaps between the segmented regions on optimized IVIM maps and reference standard were measured. Dice similarity coefficients (DS-Coeff), defined as $DS\text{-Coeffs}(A, B) = 2(A \cap B) / (A + B)$, were calculated.

Statistical Analysis

One-way analysis of variance (ANOVA) with paired measurements was used to determine differences between mean values of each IVIM parameter in each cerebral compartment. Intergroup multiple comparisons were performed between our reference standard (IVIM images derived from all 6 b values 0, 50, 100, 150, 200, 1000) and the other combinations of b values. Bland-Altman analyses were used to determine quantitative agreements between our reference standard and the other combinations of b values. One-way ANOVA with paired measurements was used to determine the differences of DS-Coeff amongst the different IVIM parameters with the same optimized b -value combinations. Statistical analyses were performed using SPSS v24.0.0 (IBM Corp, Chicago, IL, USA). For all analyses, statistical significance was set at $\alpha < 0.05$.

Results

We identified 58 patients who met our inclusion criteria, which included 36 males and 22 females with a mean age of 70.2 ± 13.4 years (range 38–93 years). Mean NIHSS at presentation was 15.9 ± 6.7 . Mean time from onset to IVIM imaging was 9.3 ± 11.7 h. Patient clinical characteristics are presented in Table 3.

According to one-way ANOVA analyses, mean values of the IVIM parametric maps (f , D^* , fD^* , and D) were compared between all groups (reference standard and combinations 1–7) within the 3 regions of interest (core infarction, non-infarcted ischemic hemisphere, and contralateral hemisphere) (Table 4; Fig. 2). The IVIM values from combination 3 ($b=0, 50, 100, 200, 1000$) showed no significant differences ($P > 0.05$) compared to the reference standard

Table 3 Basic demographic and stroke information for the study population

	$N=58$
Female sex, n (%)	23 (39.7%)
Age, years, mean \pm SD	70.2 ± 13.4
Atrial fibrillation, n (%)	27 (46.6%)
Hypertension, n (%)	44 (75.9%)
Diabetes mellitus, n (%)	11 (19.0%)
Hyperlipidemia, n (%)	32 (55.2%)
Current smoking, n (%)	8 (13.8%)
Presentation NIHSS, mean \pm SD	15.9 ± 6.7
Time from onset to imaging, h	9.3 ± 11.7

in intergroups comparison of ANOVA, except for f in the ischemic core ($P = 0.028$).

Bland-Altman analyses demonstrated that with a decreasing number of low b values ($b < 200$ s/mm²), the deviations of signal intensities between reference standard and the other combinations became more significant. For IVIM parameter f (perfusion fraction), combination 3 ($b=0, 50, 100, 200, 1000$) was most associated with our reference standard (Fig. 3). For IVIM parameter D^* (pseudodiffusion coefficient), combination 3 ($b=0, 50, 100, 200, 1000$) and combination 2 ($b=0, 50, 150, 200, 1000$) showed the best association with the reference standard (Fig. 3). For IVIM parameter fD^* (the blood flow), combination 3 ($b=0, 50, 100, 200, 1000$) and combination 2 ($b=0, 50, 150, 200, 1000$) were most associated with our reference standard (Fig. 3). For IVIM parameter D (diffusion coefficient), combination 3 ($b=0, 50, 100, 200, 1000$) and combination 2 ($b=0, 50, 150, 200, 1000$) were most associated with our reference standard. Of all combinations with 4 b values, only combination 5 ($b=0, 50, 200, 1000$) showed moderate consistency with our reference standard (Fig. 3). Of all IVIM parameters, f and D showed good coefficients of the variation of the values between optimized IVIM maps and reference standard, while fD^* and D^* had higher variability with higher standard deviation (Supplemental Table).

Based on the results above, of all combinations with 5 b values, combination 3 showed the best correlation with the reference standard, and combination 5 was the best with 4 b values. Following the Bland-Altman analysis, combinations 3 and 5 were selected to measure the spatial overlap of ischemic regions with the standard reference.

The best voxel-based overlaps of ischemic regions were on IVIM D compared with IVIM f , IVIM D^* , or IVIM fD^* ($P < 0.01$). Its mean DS-Coeff between combination 3 and 5 and standard reference were 94.11 ± 2.74 and 93.65 ± 2.38 , respectively. There were good voxel-based overlaps on IVIM f , with mean DS-Coeff between combinations 3 and 5 and standard reference were 90.30 ± 5.91 and 85.97 ± 6.09 , respectively. Both IVIM D^* and fD^* showed fair spatial

Table 4 Comparison of mean values of different IVIM parameters with different combination of b values

	Reference stan- dard	Combination 1	Combination 2	Combination 3	Combination 4	Combination 5	Combination 6	Combination 7	P-value
<i>f</i> (%)									
Ischemic core	16.63±9.34	18.67±9.7	18.32±9.76	17.28±10.02	22.78±10.95	20.06±11.51	20.58±10.64	28.54±17.15	<0.001
Non-infarct hemi- sphere	20.61±7.35	23.00±6.74	21.57±7.35	20.74±7.46	26.06±7.10	22.55±8.27	23.84±7.47	28.55±12.27	<0.001
Contralateral Hemi- sphere	22.19±6.53	24.8±6.30	22.87±6.60	22.17±6.74	27.97±6.46	23.56±7.37	25.63±6.81	28.33±10.48	<0.001
<i>D</i> (10 ⁻³ mm ² /s)									
Ischemic core	520.3±631.2	368.6±377.3	393.7±556.1	527.8±648.0	337.9±267.9	365.1±554.6	306.1±300.7	28.79±6.54	<0.001
NON-Infarct Hemi- sphere	723.8±637.3	452.4±265.0	627.5±677.4	716.0±630.6	442.5±209.4	598.1±659.8	451.4±278.6	30.87±4.22	<0.001
Contralateral Hemi- sphere	752.4±545.8	516.9±277.9	652.2±582.4	721.3±482.3	449.9±200.4	616.2±541.9	483.7±281.7	31.57±3.36	<0.001
<i>fD</i> (10 ⁻⁶ mm ² /s)									
Ischemic core	10.00±16.82	7.89±10.63	8.85±16.57	10.82±18.71	8.49±10.17	10.39±23.85	7.19±10.02	0.73±0.28	0.0028
NON-Infarct Hemi- sphere	15.45±14.63	11.03±8.5	14.7±17.26	15.73±15.62	12.07±8.07	15.12±19.59	11.52±9.52	0.84±0.26	<0.001
Contralateral Hemi- sphere	17.71±14.59	13.45±9.57	15.88±15.39	16.96±13.57	13.05±7.59	15.9±17.4	13.08±10.15	0.88±0.25	<0.001
<i>D</i> (10 ⁻⁶ mm ² /s)									
Ischemic core	558±148.3	537.5±137.4	549.3±143.4	553.9±146.4	521.6±147.6	544.7±150.9	541.6±151.8	517.6±168.5	<0.001
NON-Infarct Hemi- sphere	759.2±134.2	733.5±133.6	752.6±132.8	760.1±131.1	713.1±134	746±136.2	734.8±134.7	728.2±161.8	<0.001
Contralateral Hemi- sphere	822.3±107.5	801.7±109.0	818.8±108.8	826.5±105.9	775.7±111.2	814.3±111.1	794.1±108.5	790.0±125.8	<0.001

Texts highlighted in italics suggested there were significant differences (*P* < 0.05) when compared with the reference standard combination

Fig. 2 Comparison of different combinations of b values ROI values within different b value numbers on ischemic core. According to the inter-group multiple comparisons of ANOVA, combination 3 (b=0, 50, 100, 200, 1000) shows the best consistency with our reference standard. Of all IVIM parameters, fD^* shows the best consistency amongst the different combinations. TD also showed good consistency amongst the different combinations. Only f in the ischemic core showed significant difference amongst the different combinations. ♦ No significant differences ($P > 0.05$) when compared with reference standard of six b values within inter-group multiple comparisons

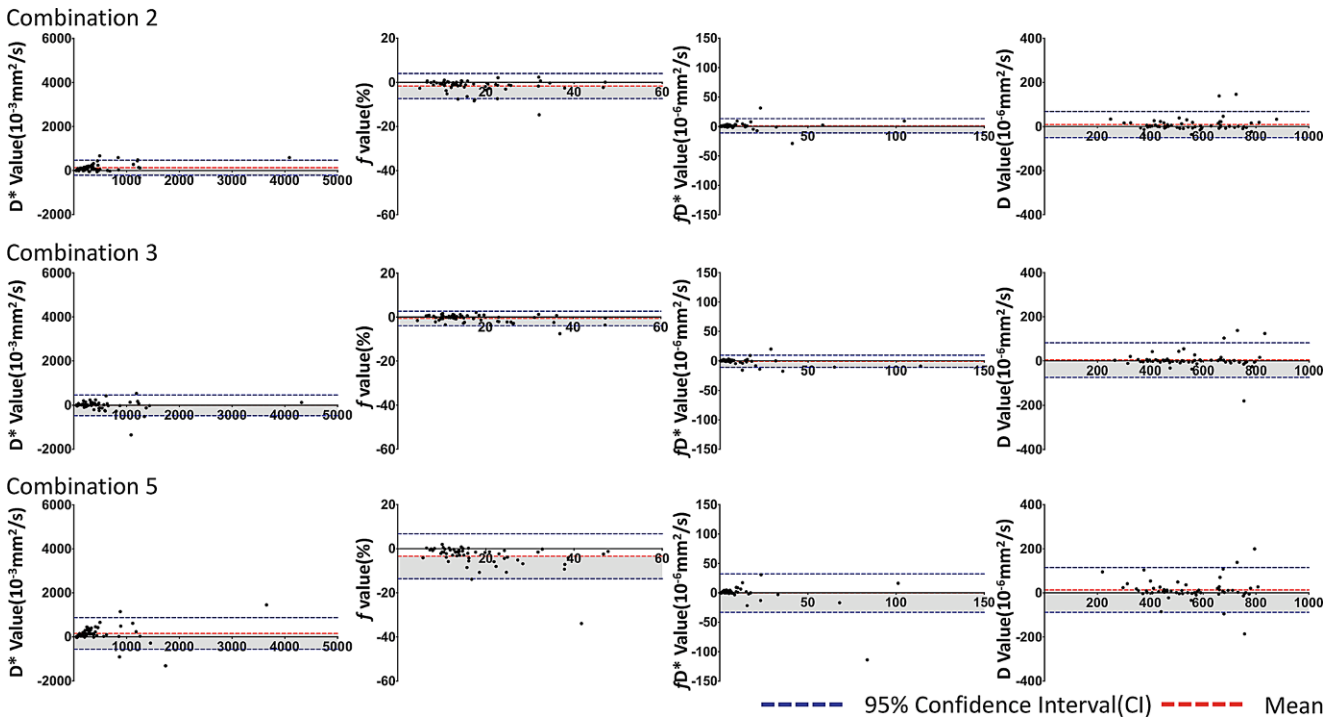
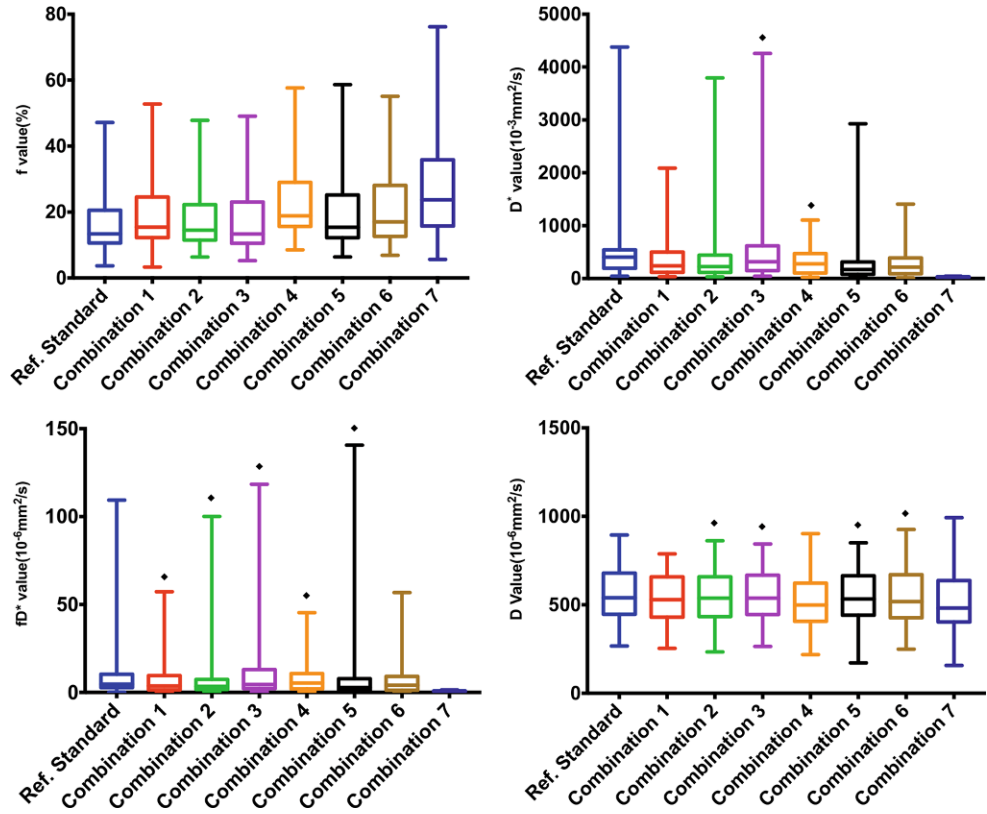


Fig. 3 Bland-Altman analyses for the regions of interest (ROI) values differences of ischemic core between reference standard combination and selected tested combinations. Bland-Altman analysis shows minimal differences in terms of IVIM values between combination 3 (b=0, 50, 100, 200, 1000) and the reference standard, indicating the best consistency. There was also good consistency between combination 2 (b=0, 50, 150, 200, 1000) and the reference standard. Although all IVIM parameters showed good consistency in combinations 3 and 2, fD^* showed the best consistency. D also showed good consistency but with more scattered values

Table 5 Voxel-based overlaps of ischemic regions between optimized IVIM maps and standard reference

	DS-Coeff with standard reference				P-value
	<i>f</i>	<i>D</i> *	<i>fD</i> *	<i>D</i>	
Combination-3	90.30 ± 5.91	80.06 ± 6.28	85.82 ± 6.52	94.11 ± 2.74	<i>P</i> < 0.01
Combination-5	85.97 ± 6.09	74.72 ± 6.35	81.05 ± 6.05	93.65 ± 2.38	<i>P</i> < 0.01

overlaps between combination 3 and 5 and standard reference (Table 5).

In general, the quality of IVIM maps decreased with a decreasing number of b values. The output images from combination 3 (b=0, 50, 100, 200, 1000), combination 2 (b=0, 50, 150, 200, 1000), and combination 5 (b=0, 50, 200, 1000) had the best quality and consistency with our reference standard (Fig. 4).

Cumulative consideration of these results shows that the minimum number of b values that showed agreement with the reference standard was combination 5 (b=0, 50, 200, 1000s/mm²).

Discussion

This study found that IVIM with 4 b values (0, 50, 200, 1000s/mm²) agrees well with a longer protocol including 6 b values (0, 50, 100, 150, 200, 1000s/mm²) for evaluation of cerebral infarction and cerebral perfusion in patients with AIS due to LVO, but at the cost of a reduced image quality. As expected, when the number of b values decreased, the values of the IVIM parameters drifted away from the reference standard values, especially for *D**, but also for *f* and *fD**. Fewer b values also resulted in significantly worse voxel-based overlap with standard reference, especially for *D** and *fD**. This finding is in agreement with previous reports [12]. The analysis revealed that acceptable IVIM values can be obtained when a b value of 50s/mm² is added to the basic 0, 200 and 1000 b values. Thus, these results suggest that lower b values around b=50s/mm² are

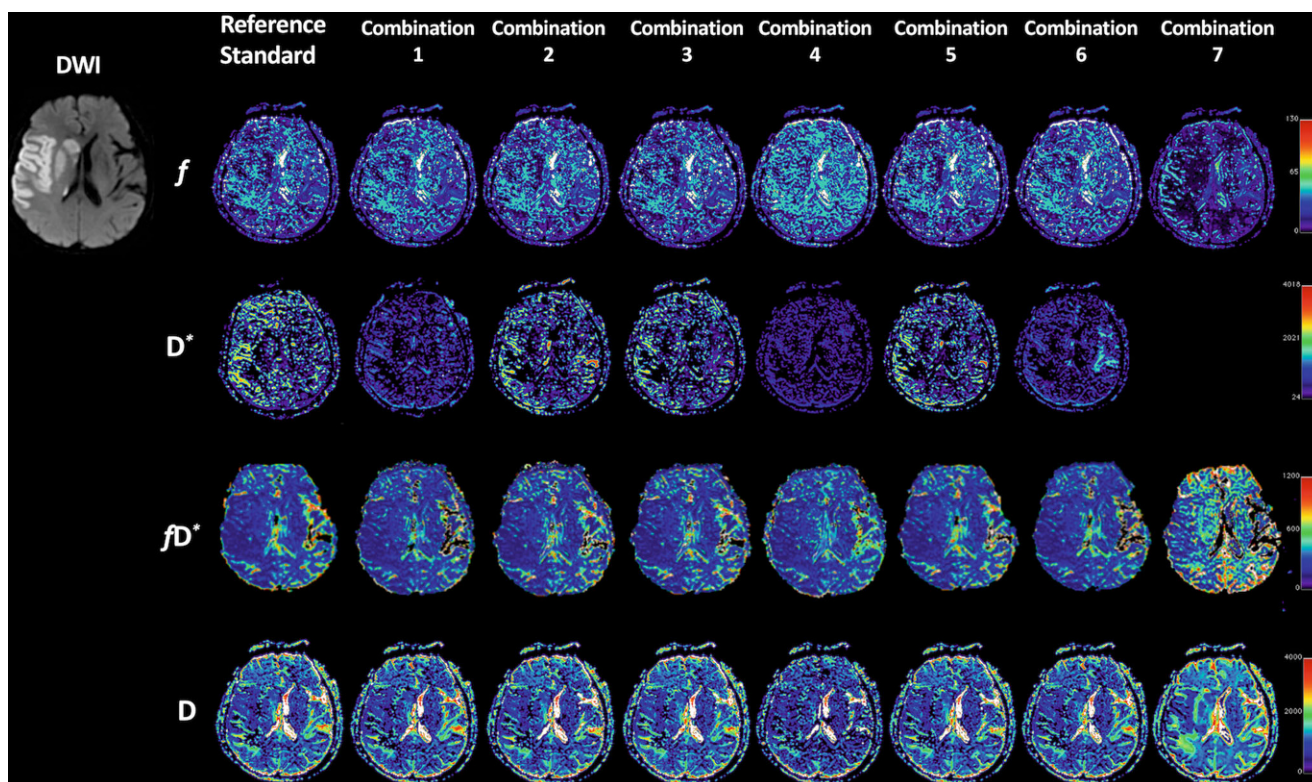


Fig. 4 A sample case to demonstrate the differences of output IVIM images among different combinations of b values. A 74-year-old female patient with acute ischemic stroke due to a right MCA artery occlusion. MRI performed after endovascular treatment triage (25h after symptom onset), demonstrated a large ischemic core. The quality of output IVIM maps decreased when the number of b values decreases especially in combinations with three b values and for *D**. There is no visible output imaging of IVIM *D** with these b values. The IVIM parametric maps from combination 3 (b=0, 50, 100, 200, 1000) and combination 2 (b=0, 50, 150, 200, 1000) show the best consistencies with the reference standard combination. Of all combinations with 4 b values, the IVIM parametric maps from combination 5 (b=0, 50, 200, 1000) have the best quality

more important compared to $50 \text{ s/mm}^2 < b < 200 \text{ s/mm}^2$ for cerebral perfusion assessment in the setting of ischemia and that IVIM MRI scan time may be reduced slightly during the imaging evaluation of AIS patients.

Patients with suspected ischemic stroke due to LVO require expeditious imaging triage to determine the size of the core infarction, whether there is salvageable brain tissue (the penumbra), and to confirm the presence of an LVO [13]. Patients with a small core infarction, salvageable brain tissue, and a large vessel occlusion are considered candidates for endovascular thrombectomy, which has been shown to lead to markedly improved clinical outcomes [14–21]. Standard rapid MRI protocols identify the core infarction with DWI, the salvageable penumbra with PWI or arterial spin labelling, and an LVO with MRA. The IVIM imaging is highly applicable to ischemic stroke given its ability to identify both core infarction and cerebral perfusion (penumbra) in a single sequence [2–5, 22]. The additional cerebral perfusion information provided by IVIM is obtained with minimal additional scan time compared to a standard DWI sequence, which is a distinct advantage compared to PWI or arterial spin labelling, which require longer acquisition times in addition to DWI.

Despite promising early results with IVIM in the context of AIS, there is little consensus on the optimal IVIM technique, including the optimal combination of b values [7, 23, 24]. Some studies suggested that IVIM perfusion information for common brain pathologies can be obtained using simplified linear fitting of as few as two nonzero b-values [25, 26]. These studies focused on D and f based on linear fitting modelling, which can be performed using a set of high b values ($>200 \text{ s/mm}^2$). The IVIM parameters D^* and fD^* are extracted predominantly from low b-values ($<200 \text{ s/mm}^2$) [23]. The suggestion that IVIM effects disappear for b values above 250 s/mm^2 implies that a biexponential fitting model with denser sampling at low b-values up to 200 s/mm^2 may best evaluate cerebral microperfusion. Fournet et al. compared monoexponential and biexponential IVIM models in rats with acute ischemic stroke. They demonstrated the advantages of biexponential models on reflecting the presence of two separate vascular pools: capillaries and larger vessels [27]. Keil et al. compared three different models including monoexponential, biexponential, and novel nonnegative least squares fittings to identify brain lesions, but this study focused mainly on brain tumors rather than AIS [12].

According to a previous study, IVIM with 6 b values ($b=0, 50, 100, 150, 200, 1000 \text{ s/mm}^2$) can detect cerebral ischemia and vasospasm [28]. This study started with six b values to identify the minimum number of b values. Many other studies also have focused on identifying the optimal b values for cerebral pathology assessment. Lemke et al. suggested that optimal measurement of IVIM parameters

involves using b values in the range of 0–360 and around 1200. In that study, 16 b-values were tested, and the use of at least 10 b-values was recommended [8]. Although the study of Lemke et al. did not determine the specific number and necessary b values for cerebral perfusion measurement, the first 4 b-values suggested by Lemke et al. [8] almost coincide with the optimal b-value set reported in the present study. By contrast, other studies have suggested the use of very different combinations of b values. Pavilla et al. measured induced hypoperfusion in brain of healthy volunteers with a fast (4 min duration) IVIM protocol that included 7 b-values (0, 60, 80, 300, 400, 900, and 1000 s/mm^2) [29]. Nelander et al. assessed cerebral perfusion in patients with pre-eclampsia with IVIM using 8 b values (0, 50, 100, 150, 200, 400, 600, 800 s/mm^2) [30]. Zhang et al. used IVIM with 15 b values ($b=0, 5, 7, 10, 15, 20, 30, 40, 50, 60, 100, 200, 400, 700, \text{ and } 1000 \text{ s/mm}^2$) to examine microvascular perfusion and microstructural integrity in patients with small cerebral vascular disease [31]. Detsky et al. used IVIM with 6 b values ($b=0, 200, 400, 600, 800, 1000 \text{ s/mm}^2$) to differentiate radiation necrosis from tumor progression in brain metastases treated with radiotherapy [32]. Thus, there is a wide variety of IVIM techniques and b values used for the measurement of cerebral perfusion and the detection of cerebral pathology.

There are several limitations to the present study. The study was retrospective in nature, and it involved acute stroke patients up to 72 h after symptom onset. Some of the patients received thrombectomy treatment before the acquisition of IVIM imaging. There may have been no or only minor hypoperfusion present for those patients, so it is not clear what optimal set-up of b values is required to identify penumbra from the ischemic core. Also, in line with a previous study [22], because IVIM output images continue to suffer from excess noise and a relatively narrow window width, it was unable to differentiate the ischemic core and the penumbra, especially in the areas with extremely low perfusion. The whole ischemic area was used on IVIM maps to determine the voxel-based overlaps. The study was performed on a single type of MRI scanner at a single institution. A large but limited number of combinations of b values were tested.

Conclusion

The IVIM imaging acquisition requires a minimum of 4 b values, with the optimal 4 b values being 0, 50, 200, 1000 s/mm^2 and IVIM with these 4 b values allows both diffusion and perfusion information to be gathered from a single short MRI sequence, which may have important implications for the imaging of AIS patients.

Author Contribution G. Zhu: drafting the article, analysis and interpretation; J. J. Heit: study conception and design, interpretation, revising the article; B. W. Martin: data acquisition and analysis; D. G. Marcellus: data acquisition and analysis; C. Federau: interpretation and revising the article; M. Wintermark: study conception and design, interpretation, revising the article.

Compliance with ethical guidelines

Conflict of interest G. Zhu, J.J. Heit, B.W. Martin, D.G. Marcellus, C. Federau and M. Wintermark declare no relationships with any companies, whose products or services may be related to the subject matter of the article.

Ethical standards For this article no studies with human participants or animals were performed by any of the authors. Written informed consent was waived by the Institutional Review Board. Institutional Review Board approval was obtained.

References

- Rydhög AS, Szczepankiewicz F, Wirestam R, Ahlgren A, Westin CF, Knutsson L, Pasternak O. Separating blood and water: perfusion and free water elimination from diffusion MRI in the human brain. *Neuroimage*. 2016;156:423–34.
- Gao QQ, Lu SS, Xu XQ, Wu CJ, Liu XL, Liu S, Shi HB. Quantitative assessment of hyperacute cerebral infarction with intravoxel incoherent motion MR imaging: initial experience in a canine stroke model. *J Magn Reson Imaging*. 2017;46:550–6.
- Hu LB, Hong N, Zhu WZ. Quantitative measurement of cerebral perfusion with Intravoxel incoherent motion in acute Ischemia stroke: initial clinical experience. *Chin Med J (Engl)*. 2015;128:2565–9.
- Suo S, Cao M, Zhu W, Li L, Li J, Shen F, Zu J, Zhou Z, Zhuang Z, Qu J, Chen Z, Xu J. Stroke assessment with intravoxel incoherent motion diffusion-weighted MRI. *NMR Biomed*. 2016;29:320–8.
- Federau C, Sumer S, Becce F, Maeder P, O'Brien K, Meuli R, Wintermark M. Intravoxel incoherent motion perfusion imaging in acute stroke: Initial clinical experience. *Neuroradiology*. 2014;56:629–35.
- Federau C, O'Brien K, Meuli R, Hagmann P, Maeder P. Measuring brain perfusion with intravoxel incoherent motion (IVIM): initial clinical experience. *J Magn Reson Imaging*. 2014;39:624–32.
- Iima M, Le Bihan D. Clinical Intravoxel incoherent motion and diffusion MR imaging: past, present, and future. *Radiology*. 2016;278:13–32.
- Lemke A, Stieltjes B, Schad LR, Laun FB. Toward an optimal distribution of b values for intravoxel incoherent motion imaging. *Magn Reson Imaging*. 2011;29:766–76.
- Federau C, Maeder P, O'Brien K, Browaeys P, Meuli R, Hagmann P. Quantitative measurement of brain perfusion with intravoxel incoherent motion MR imaging. *Radiology*. 2012;265:874–81.
- Straka M, Albers GW, Bammer R. Real-time diffusion-perfusion mismatch analysis in acute stroke. *J Magn Reson Imaging*. 2010;32:1024–37.
- Schneider CA, Rasband WS, Eliceiri KW. NIH Image to ImageJ: 25 years of image analysis. *Nat Methods*. 2012;9:671–5.
- Keil VC, Mädler B, Gielen GH, Pintea B, Hiththiya K, Gaspranova AR, Gieseke J, Simon M, Schild HH, Hadizadeh DR. Intravoxel incoherent motion MRI in the brain: Impact of the fitting model on perfusion fraction and lesion differentiability. *J Magn Reson Imaging*. 2017;46:1187–99.
- Heit JJ, Wintermark M. Imaging selection for reperfusion therapy in acute Ischemic stroke. *Curr Treat Options Neurol*. 2015;17:332.
- Albers GW, Marks MP, Kemp S, Christensen S, Tsai JP, Ortega-Gutierrez S, McTaggart RA, Torbey MT, Kim-Tenser M, Leslie-Mazwi T, Sarraj A, Kasner SE, Ansari SA, Yeatts SD, Hamilton S, Mlynash M, Heit JJ, Zaharchuk G, Kim S, Carrozella J, Palesch YY, Demchuk AM, Bammer R, Lavori PW, Broderick JP, Lansberg MG; DEFUSE 3 Investigators. Thrombectomy for stroke at 6 to 16 hours with selection by perfusion imaging. *N Engl J Med*. 2018;378:708–18.
- Berkhemer OA, Fransen PS, Beumer D, van den Berg LA, Lingsma HF, Yoo AJ, Schonewille WJ, Vos JA, Nederkoorn PJ, Wermer MJ, van Walderveen MA, Staals J, Hofmeijer J, van Oostayen JA, Lycklama à Nijeholt GJ, Boiten J, Brouwer PA, Emmer BJ, de Bruijn SF, van Dijk LC, Kappelle LJ, Lo RH, van Dijk EJ, de Vries J, de Kort PL, van Rooij WJ, van den Berg JS, van Hasselt BA, Aerden LA, Dallinga RJ, Visser MC, Bot JC, Vroomen PC, Eshghi O, Schreuder TH, Heijboer RJ, Keizer K, Tielbeek AV, den Hertog HM, Gerrits DG, van den Berg-Vos RM, Karas GB, Steyerberg EW, Flach HZ, Marquering HA, Sprengers ME, Jenniskens SF, Beenen LF, van den Berg R, Koudstaal PJ, van Zwam WH, Roos YB, van der Lugt A, van Oostenbrugge RJ, Majoie CB, Dippel DW; MR CLEAN Investigators. A randomized trial of Intraarterial treatment for acute Ischemic stroke. *N Engl J Med*. 2015;372:11–20.
- Campbell BC, Mitchell PJ, Kleinig TJ, Dewey HM, Churilov L, Yassi N, Yan B, Dowling RJ, Parsons MW, Oxley TJ, Wu TY, Brooks M, Simpson MA, Miteff F, Levi CR, Krause M, Harrington TJ, Faulder K, Steinfort BS, Priglinger M, Ang T, Scroop R, Barber PA, McGuinness B, Wijeratne T, Phan TG, Chong W, Chandraratna RV, Bladin CF, Badve M, Rice H, de Villiers L, Ma H, Desmond PM, Donnan GA, Davis SM; EXTEND-IA Investigators. Endovascular therapy for Ischemic stroke with perfusion-imaging selection. *N Engl J Med*. 2015;372:1009–18.
- Jovin TG, Chamorro A, Cobo E, de Miquel MA, Molina CA, Rovira A, San Román L, Serena J, Abilleira S, Ribó M, Millán M, Urra X, Cardona P, López-Cancio E, Tomasello A, Castaño C, Blasco J, Aja L, Dorado L, Quesada H, Rubiera M, Hernandez-Pérez M, Goyal M, Demchuk AM, von Kummer R, Gallofré M, Dávalos A; REVASCAT Trial Investigators. Thrombectomy within 8 hours after symptom onset in Ischemic stroke. *N Engl J Med*. 2015;372:2296–306.
- Goyal M, Demchuk AM, Menon BK, Eesa M, Rempel JL, Thornton J, Roy D, Jovin TG, Willinsky RA, Sapkota BL, Dowlatshahi D, Frei DF, Kamal NR, Montanera WJ, Poppe AY, Ryckborst KJ, Silver FL, Shuaib A, Tampieri D, Williams D, Bang OY, Baxter BW, Burns PA, Choe H, Heo JH, Holmstedt CA, Jankowitz B, Kelly M, Linares G, Mandzia JL, Shankar J, Sohn SI, Swartz RH, Barber PA, Coutts SB, Smith EE, Morrish WF, Weill A, Subramaniam S, Mitha AP, Wong JH, Lowerison MW, Sajobi TT, Hill MD; ESCAPE Trial Investigators. Randomized assessment of rapid Endovascular treatment of Ischemic stroke. *N Engl J Med*. 2015;372:1019–30.
- Nogueira RG, Jadhav AP, Haussen DC, Bonafe A, Budzik RF, Bhuva P, Yavagal DR, Ribo M, Cognard C, Hanel RA, Sila CA, Hassan AE, Millan M, Levy EI, Mitchell P, Chen M, English JD, Shah QA, Silver FL, Pereira VM, Mehta BP, Baxter BW, Abraham MG, Cardona P, Veznedaroglu E, Hellinger FR, Feng L, Kirmani JF, Lopes DK, Jankowitz BT, Frankel MR, Costalat V, Vora NA, Yoo AJ, Malik AM, Furlan AJ, Rubiera M, Aghaebrahim A, Olivot JM, Tekle WG, Shields R, Graves T, Lewis RJ, Smith WS, Liebeskind DS, Saver JL, Jovin TG; DAWN Trial Investigators. Thrombectomy 6 to 24 hours after stroke with a mismatch between deficit and infarct. *N Engl J Med*. 2018;378:11–21.
- Saver JL, Goyal M, Bonafe A, Diener HC, Levy EI, Pereira VM, Albers GW, Cognard C, Cohen DJ, Hacke W, Jansen O, Jovin TG, Mattle HP, Nogueira RG, Siddiqui AH, Yavagal DR, Baxter BW, Devlin TG, Lopes DK, Reddy VK, du Mesnil de Rochemont R, Singer OC, Jahan R; SWIFT PRIME Investigators. Stent-retriever

- Thrombectomy after intravenous t-PA vs. t-PA alone in stroke. *N Engl J Med*. 2015;372:2285–95.
21. Saver JL, Goyal M, van der Lugt A, Menon BK, Majoie CB, Dippel DW, Campbell BC, Nogueira RG, Demchuk AM, Tomasello A, Cardona P, Devlin TG, Frei DF, du Mesnil de Rochemont R, Berkhemer OA, Jovin TG, Siddiqui AH, van Zwam WH, Davis SM, Castaño C, Sapkota BL, Fransen PS, Molina C, van Oostenbrugge RJ, Chamorro Á, Lingsma H, Silver FL, Donnan GA, Shuaib A, Brown S, Stouch B, Mitchell PJ, Davalos A, Roos YB, Hill MD; HERMES Collaborators. Time to treatment with endovascular thrombectomy and outcomes from ischemic stroke: A meta-analysis. *JAMA*. 2016;316:1279–88.
 22. Zhu G, Federau C, Wintermark M, Marcellus DG, Martin BW, Heit JJ. Comparison of MRI IVIM and MR perfusion imaging in acute ischemic stroke due to large vessel occlusion. *Int J Stroke*. 2019. Accepted.
 23. Le Bihan D. What can we see with IVIM MRI? *Neuroimage*. 2018;187:56–67.
 24. Le Bihan D. Diffusion, confusion and functional MRI. *Neuroimage*. 2012;62:1131–6.
 25. Meeus EM, Novak J, Dehghani H, Peet AC. Rapid measurement of intravoxel incoherent motion (IVIM) derived perfusion fraction for clinical magnetic resonance imaging. *MAGMA*. 2018;31:269–83.
 26. Conklin XJ, Heyn XC, Roux XM, Cerny XM, Wintermark XM, Federau XC. Validation of a simplified model for Intravoxel Incoherent Motion Perfusion Imaging of the brain. *AJNR Am J Neuroradiol*. 2016;37:2251–7.
 27. Fournet G, Li JR, Cerjanic AM, Sutton BP, Ciobanu L, Le Bihan D. A two-pool model to describe the IVIM cerebral perfusion. *J Cereb Blood Flow Metab*. 2017;37:2987–3000.
 28. Heit JJ, Wintermark M, Martin BW, Zhu G, Marks MP, Zaharchuk G, Dodd RL, Do HM, Steinberg GK, Lansberg MG, Albers GW, Federau C. Reduced intravoxel incoherent motion microvascular perfusion predicts delayed cerebral ischemia and vasospasm after aneurysm rupture. *Stroke*. 2018;49:741–5.
 29. Pavilla A, Arrigo A, Mejdoubi M, Duvauferrier R, Gambarota G, Saint-Jalmes H. Measuring cerebral Hypoperfusion induced by hyperventilation challenge with Intravoxel incoherent motion magnetic resonance imaging in healthy volunteers. *J Comput Assist Tomogr*. 2018;42:85–91.
 30. Nelander M, Hannsberger D, Sundström-Poromaa I, Bergman L, Weis J, Åkerud H, Wikström J, Wikström AK. Assessment of cerebral perfusion and edema in preeclampsia with intravoxel incoherent motion MRI. *Acta Obstet Gynecol Scand*. 2018;97:1212–8.
 31. Zhang CE, Wong SM, Uiterwijk R, Staals J, Backes WH, Hoff EI, Schreuder T, Jeukens CR, Jansen JF, van Oostenbrugge RJ. Intravoxel incoherent motion imaging in small vessel disease: microstructural integrity and Microvascular perfusion related to cognition. *Stroke*. 2017;48:658–63.
 32. Detsky JS, Keith J, Conklin J, Symons S, Myrehaug S, Sahgal A, Heyn CC, Soliman H. Differentiating radiation necrosis from tumor progression in brain metastases treated with stereotactic radiotherapy: utility of intravoxel incoherent motion perfusion MRI and correlation with histopathology. *J Neurooncol*. 2017;134(2):433–41.